THE JOURNAL OF BIOLOGICAL CHEMISTRY VOL. 291, NO. 33, pp. 17258–17270, August 12, 2016

PtdIns(3,4,5)P_3-dependent Rac Exchanger 1 (PREX1) Rac-Guanine Nucleotide Exchange Factor (GEF) Activity Promotes Breast Cancer Cell Proliferation and Tumor Growth via Activation of Extracellular Signal-regulated Kinase 1/2 (ERK1/2) Signaling*

Received for publication, June 12, 2016 Published, JBC Papers in Press, June 29, 2016, DOI 10.1074/jbc.M116.743401

Heng-Jia Liu[‡], Lisa M. Ooms[‡], Nuthasuda Srijakotre[‡], Joey Man[‡], Jessica Vieusseux[‡], JoAnne E. Waters[‡], Yue Feng[§], Charles G. Bailey[§¶], John E. J. Rasko[‡¶‖], John T. Price[‡], and Christina A. Mitchell[‡1]**

*From the [‡]Cancer Program, Monash Biomedicine Discovery Institute, and Department of Biochemistry and Molecular Biology, Monash University, Victoria 3800, Australia, the [§]Centenary Institute of Cancer Medicine and Cell Biology, New South Wales 2050, Australia, [¶]Sydney Medical School, University of Sydney, Sydney, New South Wales 2006, Australia, [‖]Cell and Molecular Therapies, Royal Prince Alfred Hospital, Camperdown, New South Wales 2050, Australia, and the **Centre for Chronic Disease, College of Health and Biomedicine, Victoria University, Victoria 8001, Australia*

PtdIns(3,4,5)P_3-dependent Rac exchanger 1 (PREX1) is a Rac-guanine nucleotide exchange factor (GEF) overexpressed in a significant proportion of human breast cancers that integrates signals from upstream ErbB2/3 and CXCR4 membrane surface receptors. However, the PREX1 domains that facilitate its oncogenic activity and downstream signaling are not completely understood. We identify that ERK1/2 MAPK acts downstream of PREX1 and contributes to PREX1-mediated anchorage-independent cell growth. PREX1 overexpression increased but its shRNA knockdown decreased ERK1/2 phosphorylation in response to EGF/IGF-1 stimulation, resulting in induction of the cell cycle regulators cyclin D1 and p21$^{WAF1/CIP1}$. PREX1-mediated ERK1/2 phosphorylation, anchorage-independent cell growth, and cell migration were suppressed by inhibition of MEK1/2/ERK1/2 signaling. PREX1 overexpression reduced staurosporine-induced apoptosis whereas its shRNA knockdown promoted apoptosis in response to staurosporine or the anti-estrogen drug tamoxifen. Expression of wild-type but not GEF-inactive PREX1 increased anchorage-independent cell growth. In addition, mouse xenograft studies revealed that expression of wild-type but not GEF-dead PREX1 resulted in the formation of larger tumors that displayed increased phosphorylation of ERK1/2 but not AKT. The impaired anchorage-independent cell growth, apoptosis, and ERK1/2 signaling observed in stable *PREX1* knockdown cells was restored by expression of wild-type but not GEF-dead-PREX1. Therefore, PREX1-Rac-GEF activity is critical for PREX1-dependent anchorage-independent cell growth and xenograft tumor growth and may represent a possible therapeutic target for breast cancers that exhibit PREX1 overexpression.

The Rac proteins (Rac1, Rac2, and Rac3) are a subgroup of the Rho-GTPase family that regulate cell motility and, when deregulated, drive cancer invasion and metastasis (1–3). Rac proteins undergo rapid and spatiotemporally coordinated cycles of activation and inactivation linked to upstream receptor signaling by guanine nucleotide exchange factors (GEFs)[2] (4). The most common mechanism for Rac hyperactivation in human cancer is via dysregulation of Rac-GEF activity. PtdIns (3,4,5)P_3-dependent Rac exchanger 1 (PREX1) is a member of the *Dbl* family of Rho-GEFs that promotes chemoattractant-stimulated neutrophil chemotaxis and reactive O_2 species formation (5–7). PREX1 is a multidomain protein that contains an N-terminal catalytic Dbl-homologous (DH) domain, which activates Rac, adjacent to a pleckstrin homology (PH) domain, which binds to and is activated by PI3K-generated PtdIns(3,4,5)P_3, followed by two dishevelled, EGL-10 and pleckstrin (DEP) domains, two PDZ domains, and a catalytically inactive C-terminal inositol polyphosphate 4-phosphatase (IP4P) domain, which shares 30% amino acid identity with the catalytically active IP4P domain of the inositol polyphosphate 4-phosphatases INPP4A and INPP4B (5, 8, 9). The IP4P domain of PREX1 contains a common catalytic CX_5R motif shared by dual specificity phosphoinositide phosphatases; however, PREX1 does not exhibit phosphatase activity for unknown reasons (5). PREX1 is synergistically activated by PtdIns(3,4,5)P_3 generated by PI3K and the $\beta\gamma$ subunits of G-protein-coupled receptors (5, 8).

PREX1 and the related PREX2 were recently identified as putative oncogenes in human cancers (10–14). The human *PREX1* gene is located on chromosome 20q13, and amplification of this region occurs in 8–29% of breast tumors associated with a poor prognosis (10). This region is also frequently deleted or amplified in malignant myeloid diseases (15), hered-

* This work was supported by a grant from the National Health and Medical Research Council (APP1044737) and a fellowship and research grant from Tour de Cure (to C. G. B. and J. E. J. R.). The authors declare that they have no conflicts of interest with the contents of this article.

[1] To whom correspondence should be addressed: Cancer Program, Monash Biomedicine Discovery Institute and Dept. of Biochemistry and Molecular Biology, 23 Innovation Walk, Monash University, Clayton 3800, VIC, Australia. Tel.: 61-3-9905-4318; Fax: 61-3-9594-0183; E-mail: christina.mitchell@monash.edu.

[2] The abbreviations used are: GEF, guanine nucleotide exchange factor; DH, Dbl-homologous; DEP, dishevelled, EGL-10 and pleckstrin; PtdIns(3,4,5)P_3, phosphatidylinositol (3,4,5)-trisphosphate; PARP, poly (ADP-ribose) polymerase I; PH, pleckstrin homology; IP4P, inositol polyphosphate 4-phosphatase; MTT, 3-(4,5-dimethylthiazol-2-yl)-2,5-diphenyltetrazolium bromide.

itary prostate cancer (16), pancreatic endocrine tumors (17), and ovarian cancers (18). PREX1 expression is not detected in the normal breast; however, the *PREX1* gene is amplified in primary breast tumors, with PREX1-positive staining observed by immunohistochemistry in 58% of breast cancers (10). In particular *PREX1* mRNA and protein levels are up-regulated in ER^+/luminal breast tumors (10, 19). Higher *PREX1* mRNA expression has also been reported in $ErbB2^+$ tumors in one study (10). In breast cancer cells, neuregulin activation of ErbB receptors results in PREX1 phosphorylation, increasing its Rac-GEF activity (11). PREX1 converges signals from ErbB receptors and G-protein-coupled receptors. Ectopic PREX1 expression in cultured cells promotes cell viability, migration, and invasion (19, 20). In contrast *PREX1* shRNA knockdown in ER^+ breast cancer cells results in reduced cell migration, proliferation, anchorage-independent cell growth, and xenograft tumor growth (10, 11). Although there is compelling evidence that PREX1 expression is increased in some breast cancer subsets and that its activation is driven by G-protein-coupled receptors and PI3K signaling (10, 11), there is very little data that reveal the mechanism of oncogenic PREX1 signaling.

Here we demonstrate that PREX1 increases cell proliferation, migration, anchorage-independent cell growth, and xenograft tumor growth by promoting ERK1/2 activation and that inhibition of ERK1/2 signaling suppresses PREX1 effects. PREX1-mediated breast cancer cell growth/survival under anchorage-independent conditions and xenograft tumor growth are critically dependent on its Rac-GEF activity, which activates ERK1/2. These studies therefore suggest that inhibition of PREX1 Rac-GEF activity may represent a therapeutic strategy for treatment of breast tumors that exhibit PREX1 overexpression.

Results

PREX1 Regulates ERK1/2 Signaling in Both ER^+ and ER^- Breast Cancer Cell Lines—EGF, IGF-1, and the ErbB2/3 ligand heregulin activate Rac1 in many breast cancer cell lines (10, 21–24). To investigate the signaling pathways regulated by PREX1 that promote cell proliferation and survival, MDA-MB-231-luc-D3H1 cells, an ER^- basal breast cancer cell line that does not exhibit PREX1 protein expression (10), were stably transduced to express full-length PREX1, which was N-terminally tagged with HA (Fig. 1*A*). MDA-MB-231-luc-D3H1 cells expressed HA-PREX1 at similar levels as endogenous PREX1 in ER^+ MCF-7-luc-F5 breast cancer cells (Fig. 1*A*). In response to EGF stimulation, AKT phosphorylation (Ser^{473}) was increased in MDA-MB-231-luc-D3H1 cells expressing PREX1 relative to vector controls, but this was not statistically significant (Fig. 1, *B* and *C*). However, a significant increase in ERK1/2 phosphorylation (Thr^{202}/Thr^{204}) was observed for up to 30 min after EGF stimulation in cells expressing PREX1 relative to vector controls (Fig. 1, *B* and *D*), and this was suppressed by treatment with a small molecule MEK1/2 inhibitor, U0126, which blocks downstream ERK1/2 activation (25, 26) (Fig. 1, *E* and *F*). To confirm that endogenous PREX1 regulates ERK1/2 activation, two distinct shRNA interference sequences were utilized to stably knock down endogenous PREX1 in ER^+ MCF-7-luc-F5 cells that express PREX1 (10), and >75% knockdown was achieved, as determined by PREX1 immunoblot (Fig. 2, *A* and *B*) and mRNA analysis (Fig. 2*C*). IGF-1 (10 ng/ml)-induced ERK1/2 phosphorylation was significantly reduced in *PREX1*-depleted cells (Fig. 2, *D* and *E*). PREX1 expression promotes AKT activation in response to IGF-1 (10 or 100 ng/ml) stimulation in MCF-7 cells (19); however, no significant change in AKT phosphorylation (Ser^{473} and Thr^{308}) was demonstrated at the concentration of IGF-1 used in our studies (10 ng/ml), although a trend toward decreased phosphorylation was observed (Fig. 2, *F–H*). These data suggest that PREX1 enhances ERK1/2 activation following EGF stimulation of ER^- or low-dose IGF-1 stimulation of ER^+ breast cancer cells.

PREX1-mediated ERK1/2 Activation Is Dependent on Its Rac-GEF Activity—PREX1 contains an N-terminal catalytic DH-PH domain, two DEP domains, two PDZ domains, and a C-terminal, ~350-amino acid region (IP4P domain) that shares ~30% amino acid identity to the PtdIns(3,4)P_2 4 phosphatases INPP4A and INPP4B (5, 8, 9) (Fig. 3*A*). The PREX1 N-terminal PH domain binds to and is activated by PtdIns(3,4,5)P_3, whereas the DH domain binds and activates Rac. The DH-PH domain is required for maximal Rac-GEF activity (5, 8), but to date the PREX1 domain(s) that facilitate its oncogenic signaling are unknown. To dissect the molecular mechanisms by which PREX1 enhances ERK1/2 activity, we stably expressed constructs encoding wild-type HA-tagged PREX1 (HA-PREX1), PREX1 that lacks the IP4P domain (HA-Δ4P-PREX1, amino acids 36–1364), the isolated IP4P domain (HA-4P-PREX1, amino acids 791–1659), or a PREX1 (E56A/N238A) "GEF-dead" mutant (GEF-dead HA-PREX1, Ref. 8) (Fig. 3*A*) in *PREX1* shRNA-depleted MCF-7-luc-F5 cells. Reconstitution of *PREX1* knockdown with wild-type HA-PREX1 restored ERK1/2 phosphorylation to levels observed in control shRNA cells following low-dose IGF-1 stimulation (10 ng/ml) (Fig. 3, *B* and *C*), which was also observed with expression of HA-Δ4P-PREX1 but not HA-4P-PREX1 (Fig. 3, *B* and *C*). Notably, expression of GEF-dead HA-PREX1 was unable to restore ERK1/2 phosphorylation to the levels observed in control shRNA cells or in *PREX1* shRNA cells expressing wild-type HA-PREX1 (Fig. 3, *B* and *C*), indicating that PREX1 Rac-GEF activity is critical for its activation of ERK1/2. In control studies, all PREX1 mutants were expressed at comparable or higher levels relative to wild-type PREX1 expression in *PREX1* shRNA cells, as assessed by anti-HA immunoblot (Fig. 3*B*).

PREX1 Regulates Cell Proliferation and Cyclin D1 and $p21^{WAF1/CIP1}$ Expression—ERK1/2 regulates G_1-S phase progression by stimulating the transcription of the proto-oncogene cyclin D1 (27, 28). Cyclin D1 enhances G_1-S phase progression by forming a complex with cyclin-dependent kinase (Cdk) 4 and Cdk6 (29). The cyclin D1-Cdk4/6 complex phosphorylates and inactivates the retinoblastoma protein, resulting in activation of the E2F transcription factor. E2F then, in turn, activates various genes required for cell cycle progression from G_1 to S phase (30). ERK1/2 also regulates G_1-S phase progression by modulating the expression of Cdk inhibitors, including $p21^{WAF1/CIP1}$ and $p27^{KIP1}$. Mitogen-induced ERK1/2 activation leads to the transient accumulation of $p21^{WAF1/CIP1}$ in early G_1 phase (31, 32). Cells with *PREX1* shRNA knockdown or overexpression showed reduced or enhanced cell proliferation,

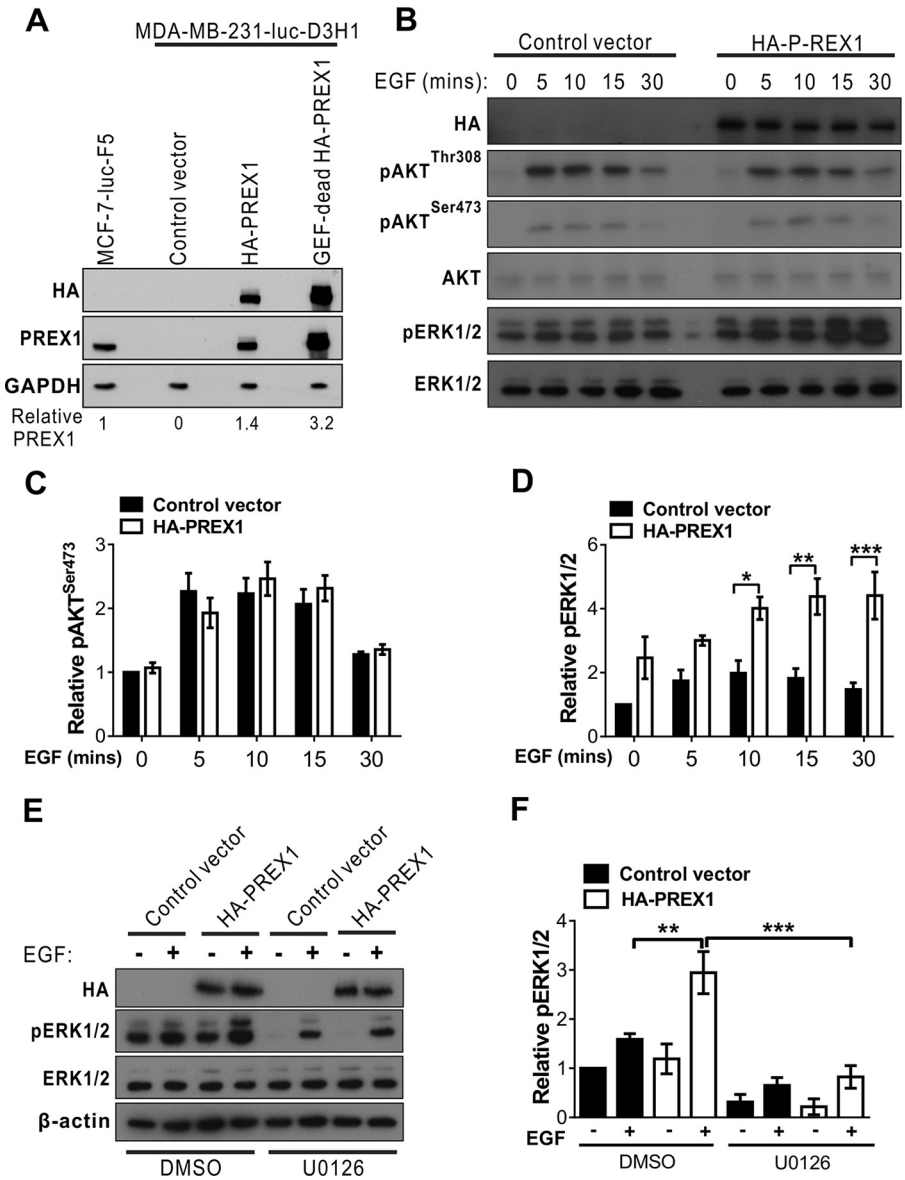

FIGURE 1. **Overexpression of PREX1 enhances ERK1/2 but not AKT phosphorylation in MDA-MB-231-luc-D3H1 cells.** *A*, MDA-MB-231-luc-D3H1 cells stably transduced with control vector, HA-PREX1, or GEF-dead HA-PREX1 and parental MCF-7-luc-F5 cells were analyzed by immunoblotting using HA, PREX1, or GAPDH antibodies. Normalized PREX1 protein expression relative to endogenous PREX1 levels in MCF-7-luc-F5 cells is shown below. *B*, cells were serum-starved for 24 h and then stimulated with 100 ng/ml EGF for the indicated time periods. Cell lysates were immunoblotted using HA, pAKT$^{Thr-308}$, pAKT$^{Ser-473}$, AKT, pERK1/2, or ERK1/2 antibodies. *C* and *D*, data are presented as mean -fold change in pAKT$^{Ser-473}$/AKT (*C*) or pERK1/2/ERK1/2 (*D*) ± S.E. relative to control vector at 0 min EGF stimulation, which was assigned an arbitrary value of 1 ($n = 3$). *E*, cells were serum-starved for 24 h, treated with 1 μM U0126 (MEK1/2 inhibitor), and stimulated with 100 ng/ml EGF for 15 min. Cell lysates were immunoblotted using HA, pERK1/2, ERK1/2, or β-actin antibodies. *F*, data are expressed as mean -fold change in pERK1/2/ERK1/2 ± S.E. relative to DMSO-treated control vector at 0 min EGF stimulation, which was assigned an arbitrary value of 1 ($n = 3$). *, $p < 0.05$; **, $p < 0.01$; ***, $p < 0.001$.

respectively, after 72 h, as demonstrated by 3-(4,5-dimethylthiazol-2-yl)-2,5-diphenyltetrazolium bromide (MTT) assays (Fig. 4, *A* and *B*). Additionally, EGF-stimulated expression of cyclin D1 and p21$^{WAF1/CIP1}$ was enhanced in PREX1-overexpressing cells (Fig. 4, *C–E*). In contrast, *PREX1* shRNA knockdown reduced cyclin D1 and p21$^{WAF1/CIP1}$ proteins levels in response to low-dose IGF-1 (10 ng/ml) stimulation (Fig. 4, *F–H*).

PREX1 Regulates Staurosporine/Tamoxifen-induced Apoptosis—To reveal the role PREX1 plays in regulating cell death, cells were treated with staurosporine, a potent stimulus frequently used to induce apoptosis in mammalian cells, including MCF-7 and MDA-MB-231 breast cancer cell lines (33–35). PREX1 overexpression in MDA-MB-231-luc-D3H1 cells significantly reduced the number of apoptotic cells (TUNEL-positive) (Fig. 5*A*) following staurosporine treatment associated with decreased cleavage of caspase-3 and poly (ADP-ribose) polymerase I (PARP) (Fig. 5, *B–D*). PREX1 regulation of staurosporine-induced apoptosis was confirmed in stable *PREX1* shRNA knockdown cells. *PREX1* depletion in MCF-7-luc-F5 cells was associated with increased staurosporine-mediated cell death (Fig. 5*E*). MCF-7 cells do not express caspase-3; therefore, only PARP cleavage was assessed. Following staurosporine treatment, *PREX1* depletion decreased intact PARP levels associated with the appearance of cleaved PARP (Fig. 5, *F* and *G*).

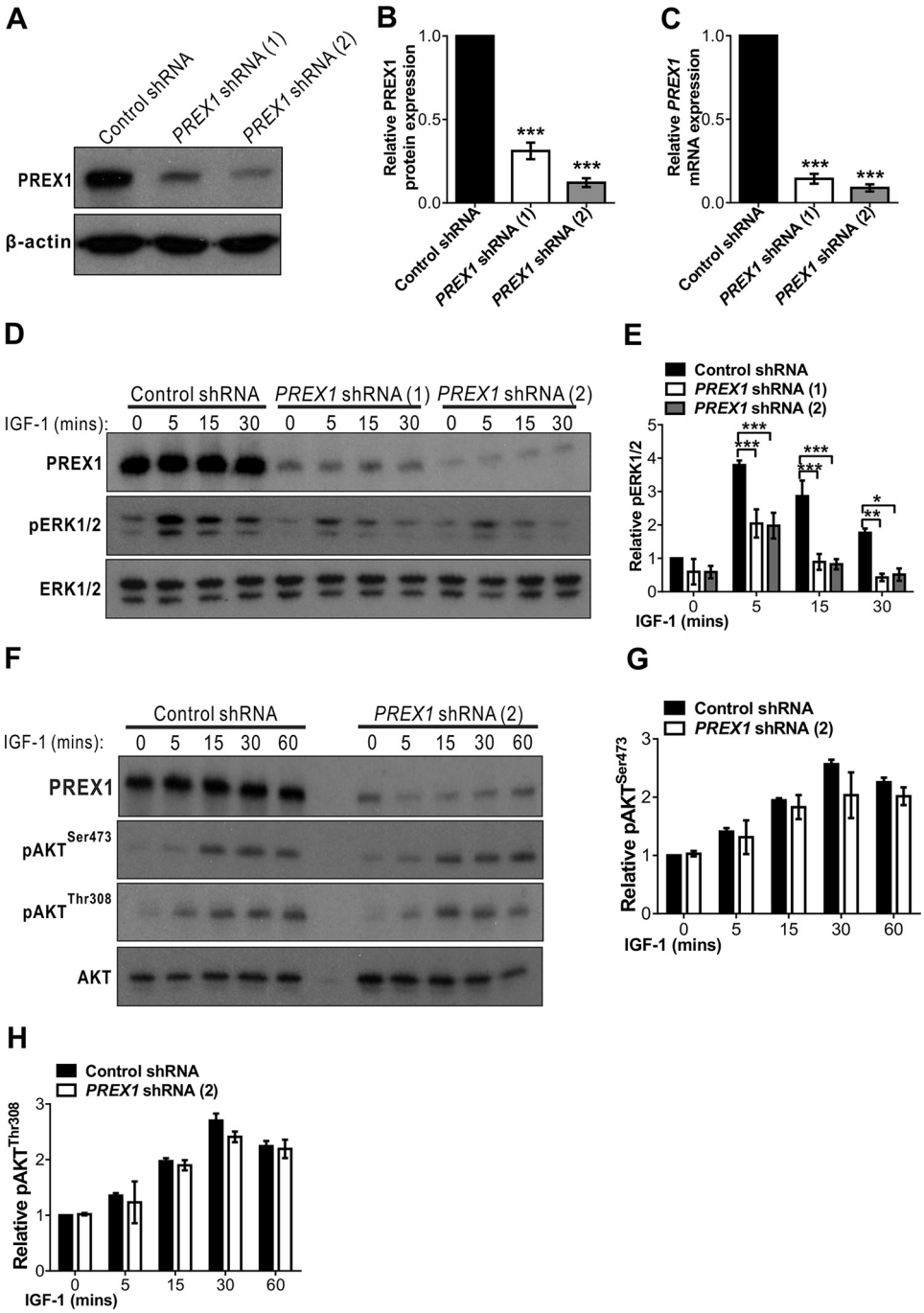

FIGURE 2. ***PREX1* knockdown decreases ERK1/2 but not AKT phosphorylation in MCF-7-luc-F5 cells.** *A*, cells stably transduced with two different *PREX1* shRNA (*PREX1* shRNA (1) and *PREX1* shRNA (2)) or a non-target control shRNA were analyzed by immunoblotting using PREX1 or β-actin antibodies. *B*, densitometric values of PREX1 expression are shown as mean ± S.E. relative to control shRNA, which was assigned an arbitrary value of 1 ($n = 3$). *C*, quantitative RT-PCR analysis of *PREX1* mRNA normalized to *GAPDH* from MCF-7-luc-F5 cells stably expressing control shRNA, *PREX1* shRNA (1), or *PREX1* shRNA (2). Data are presented as mean -fold difference ± S.E. relative to control shRNA, which was assigned an arbitrary value of 1 ($n = 3$). *D*, cells were serum-starved for 24 h and then stimulated with 10 ng/ml IGF-1 for the indicated time periods. Cell lysates were immunoblotted using PREX1, pERK1/2, or ERK1/2 antibodies. *E*, data are expressed as mean -fold change in pERK1/2/ERK1/2 ± S.E. relative to control shRNA at 0 min IGF-1 stimulation, which was assigned an arbitrary value of 1 ($n = 3$). *F*, cells were serum-starved for 24 h and then stimulated with 10 ng/ml IGF-1 for the indicated time periods. Cell lysates were immunoblotted using PREX1, $pAKT^{Ser\text{-}473}$, $pAKT^{Thr\text{-}308}$, or AKT antibodies. *G* and *H*, data are expressed as mean -fold change in $pAKT^{Ser\text{-}473}$/AKT (*G*), $pAKT^{Thr\text{-}308}$/AKT (*H*) ± S.E. relative to control shRNA at 0 min IGF-1 stimulation, which was assigned an arbitrary value of 1 ($n = 3$). *, $p < 0.05$; **, $p < 0.01$; ***, $p < 0.001$.

PREX1 knockdown did not promote PARP cleavage in the absence of staurosporine treatment, suggesting that PREX1 regulates apoptosis in response to extrinsic signals. The elevated cell death induced by staurosporine observed in *PREX1* knockdown MCF-7-luc-F5 cells was rescued by reconstitution of wild-type HA-PREX1 or HA-Δ4P-PREX1 but not GEF-dead HA-PREX1 (Fig. 5*H*), indicating that PREX1 Rac-GEF activity is critical for PREX1 regulation of staurosporine-induced apoptosis in breast cancer cells. Apoptosis can be induced in ER^+ MCF-7 breast cancer cells by treatment with tamoxifen, a

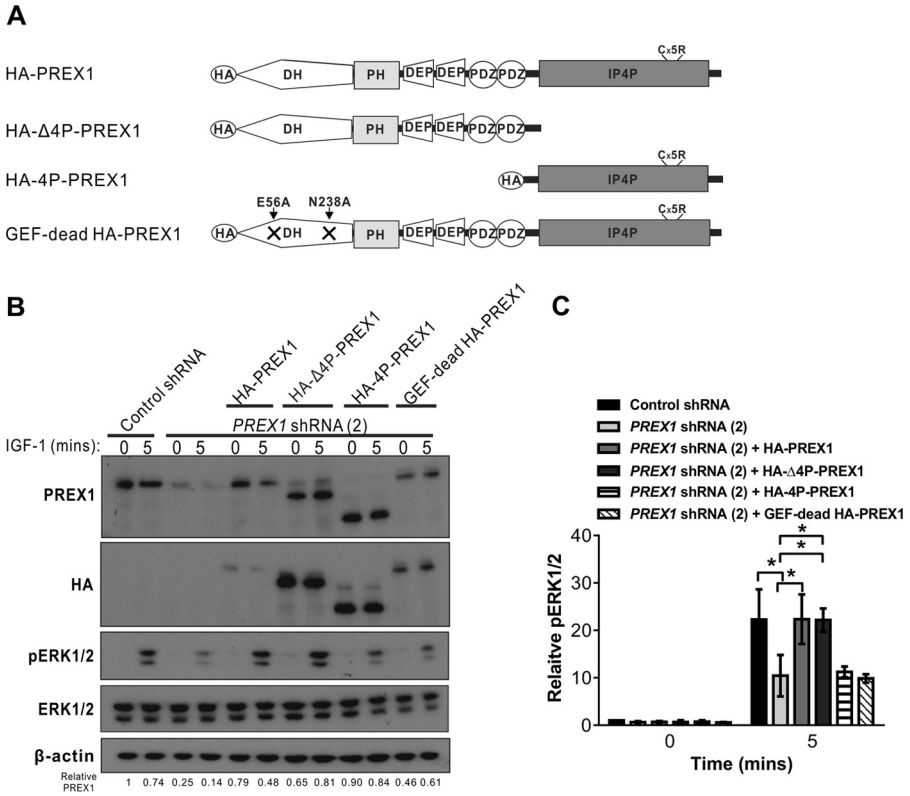

FIGURE 3. **Reconstitution of wild-type but not GEF-dead-PREX1 restores ERK1/2 activation in *PREX1* knockdown MCF-7-luc-F5 cells.** *A*, schematic of PREX1 constructs: full-length wild-type PREX1 (*HA-PREX1*), the PREX1 mutant lacking the IP4P domain but containing DH/PH/DEP-DEP/PDZ-PDZ (*HA-Δ4P-PREX1*), the PREX1 mutant containing only the IP4P domain (*HA-4P-PREX1*), and the PREX1 (E56A/N238A) GEF-dead mutant (*GEF-dead HA-PREX1*). *B*, stable MCF-7-luc-F5 cells expressing control shRNA, *PREX1* shRNA (2), *PREX1* shRNA (2) + HA-PREX1, *PREX1* shRNA (2) + HA-Δ4P-PREX1, *PREX1* shRNA (2) + HA-4P-PREX1, or *PREX1* shRNA (2) + GEF-dead HA-PREX1 were serum-starved for 24 h and then stimulated with 10 ng/ml IGF-1 for the indicated time periods. Cell lysates were immunoblotted using PREX1, HA, pERK1/2, ERK1/2, or β-actin antibodies. Normalized PREX1 protein expression relative to endogenous PREX1 levels in MCF-7-luc-F5 control shRNA cells at 0 min IGF-1 stimulation is shown below. *C*, data are expressed as mean -fold change in pERK1/2/ERK1/2 ± S.E. relative to control shRNA at 0 min IGF-1 stimulation, which was assigned an arbitrary value of 1 ($n = 3$). *, $p < 0.05$.

widely used anti-estrogen drug. *PREX1* knockdown significantly increased the number of apoptotic cells in response to tamoxifen treatment compared with control shRNA cells (Fig. 5*I*).

PREX1 Mediates Anchorage-independent Cell Growth via ERK1/2—To determine whether PREX1 regulates cell growth/survival under anchorage-independent conditions, soft agar assays were undertaken using MDA-MB-231-luc-D3H1 cells overexpressing wild-type or GEF-dead PREX1 (Fig. 1*A*). PREX1 overexpression significantly increased the number of colonies formed compared with vector controls (Fig. 6, *A* and *B*). Although GEF-dead HA-PREX1 overexpression marginally increased colony formation compared with control vector cells, expression of PREX1 lacking Rac-GEF activity did not enhance anchorage-independent cell growth to the levels observed in wild-type HA-PREX1 cells (Fig. 6, *A* and *B*). Previous studies have independently reported that ERK1/2 or PREX1/Rac1 promotes anchorage-independent growth of breast cancer cells (10, 36, 37). To determine whether PREX1 promotes anchorage independent colony formation via Rac1-ERK1/2, soft agar studies were undertaken in MDA-MB-231-luc-D3H1 cells overexpressing PREX1 in the presence of a MEK1/2 inhibitor (U0126), Rac1 inhibitor (NSC23766), or DMSO (vehicle). Colony formation was significantly reduced in a dose-dependent manner in PREX1-overexpressing cells in the presence of NSC23766 (Fig. 6, *C* and *D*). Furthermore, treatment with U0126 significantly reduced colony formation in HA-PREX1-overexpressing cells to the levels observed in control cells (Fig. 6, *E* and *F*). Therefore, PREX1-enhanced anchorage-independent cell growth is dependent on Rac1 and ERK1/2. In contrast, *PREX1* shRNA knockdown reduced the number of colonies formed in soft agar, as reported previously (Fig. 6, *G* and *H*) (10, 11). The impaired anchorage-independent cell growth observed in stable *PREX1* knockdown cells was restored by expression of wild-type HA-PREX1 but not GEF-dead HA-PREX1 (Fig. 6, *G* and *H*), indicating that the ability of PREX1 to promote anchorage-independent cell growth is dependent on its Rac-GEF activity.

PREX1 Promotes Cell Migration via ERK1/2—PREX1 and ERK1/2 have both been independently shown to promote cancer cell migration (10, 13, 38, 39). Our results suggest that ERK1/2 signaling is an important downstream mediator of PREX1 function in breast cancer cells. We therefore investigated whether ERK1/2 signaling contributes to PREX1-mediated cell migration using Transwell Boyden chamber migration assays. Overexpression of PREX1 in MDA-MB-231-luc-D3H1 cells significantly enhanced the migration of cells toward 10% serum relative to vector controls (Fig. 6, *I* and *J*). Inhibition of ERK1/2 activity using U0126 significantly suppressed the migration of PREX1-overexpressing

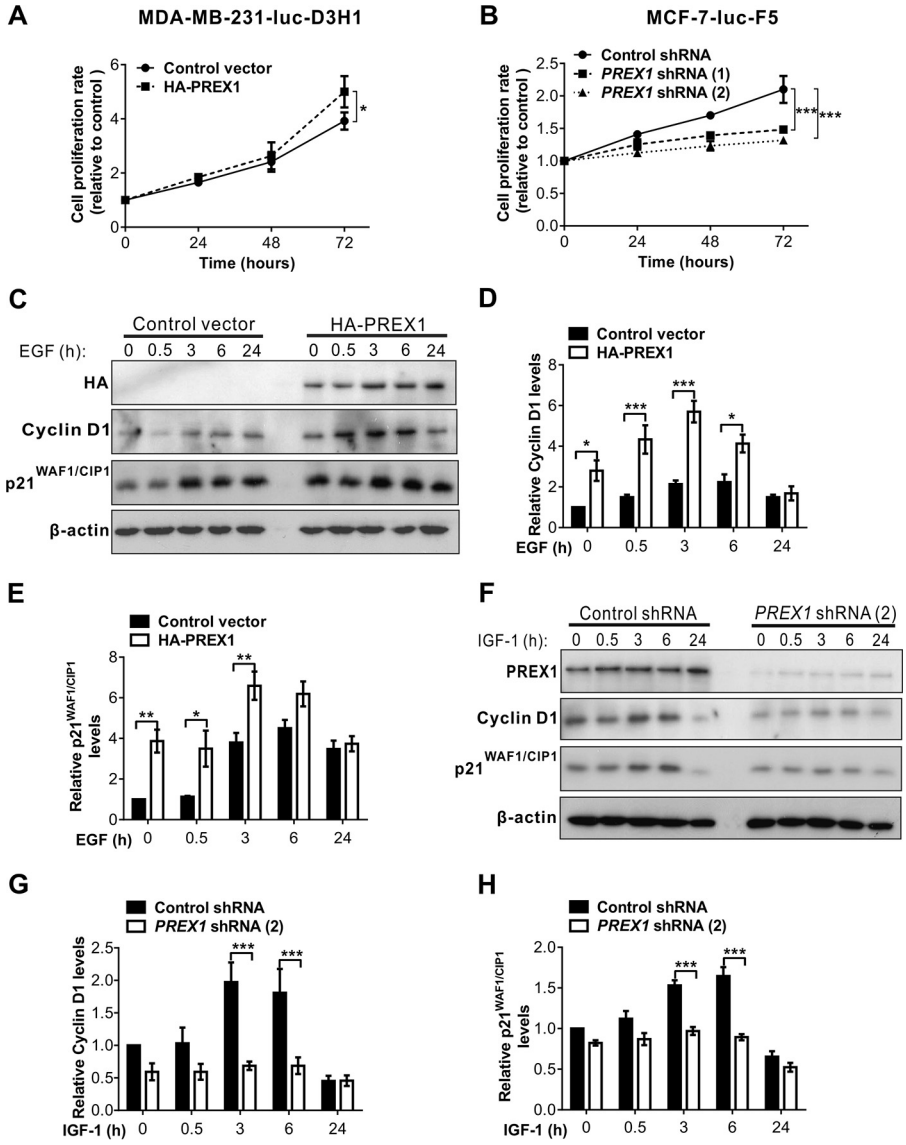

FIGURE 4. **PREX1 regulates cell proliferation and cyclin D1/p21$^{WAF1/CIP1}$ induction.** *A* and *B*, MTT proliferation assays were performed on stable MDA-MB-231-luc-D3H1 cells expressing control vector or HA-PREX1 (*A*) or stable MCF-7-luc-F5 cells expressing control shRNA, *PREX1* shRNA (1), or *PREX1* shRNA (2) (*B*). Data points represent the relative mean cell proliferation ± S.E. relative to control, which was assigned an arbitrary value of 1 ($n = 5$). *C*, MDA-MB-231-luc-D3H1 cells were serum-starved for 24 h and then stimulated with 100 ng/ml EGF for the time periods as indicated. Cell lysates were immunoblotted using HA, cyclin D1, p21$^{WAF1/CIP1}$, or β-actin antibodies. *D* and *E*, densitometric values of cyclin D1 (*D*) or p21$^{WAF1/CIP1}$ (*E*) were normalized to β-actin. Data are expressed as mean -fold difference ± S.E. relative to control vector at 0 min EGF stimulation, which was assigned an arbitrary value of 1 ($n = 3$). *F*, MCF-7-luc-F5 cells were serum-starved for 24 h and then stimulated with 10 ng/ml IGF-1 for the indicated time periods. Cell lysates were immunoblotted using PREX1, cyclin D1, p21$^{WAF1/CIP1}$, or β-actin antibodies. *G* and H, densitometric values of cyclin D1 (*G*) or p21$^{WAF1/CIP1}$ (*H*) were normalized to β-actin. Data are expressed as mean -fold difference ± S.E. relative to control shRNA at 0 min EGF stimulation, which was assigned an arbitrary value of 1 ($n = 3$). *, $p < 0.05$; **, $p < 0.01$; ***, $p < 0.001$.

cells to the levels observed in vehicle-treated vector controls (Fig. 6, *I* and *J*), indicating that inhibition of ERK1/2 activity is sufficient to disrupt the enhanced migratory capacity induced by PREX1 overexpression.

PREX1 Promotes Xenograft Tumor Growth—To determine the effects of PREX1 overexpression on tumorigenesis *in vivo*, we conducted xenograft studies in nude mice. MDA-MB-231-luc-D3H1 cells overexpressing wild-type or GEF-dead PREX1 or vector controls (Fig. 7*A*) were injected into the inguinal mammary fat pads of BALB/c nude mice, and orthotopic mammary xenograft growth was analyzed 12 days after surgery. Although *PREX1* shRNA-mediated depletion has been reported to suppress xenograft tumor growth (10, 11), the effects of PREX1 overexpression, which recapitulates the increased expression observed in some human breast cancers, has not been reported. Wild-type, but not GEF-dead, PREX1 overexpression significantly increased the growth of xenograft tumors formed by MDA-MB-231-luc-D3H1 cells compared with vector controls (Fig. 7, *B–D*). Histopathological analysis demonstrated increased cell proliferation and reduced cell death, as shown by Ki-67 and cleaved caspase-3 staining, respectively, in PREX1-overexpressing tumors (Fig. 7, *E–G*). PREX1-overexpressing tumors also showed evidence of increased expression of activated (phosphorylated) ERK1/2 relative to controls, as shown by phosphospecific antibody staining; however, no change in the intensity of pAKT$^{Ser-473}$

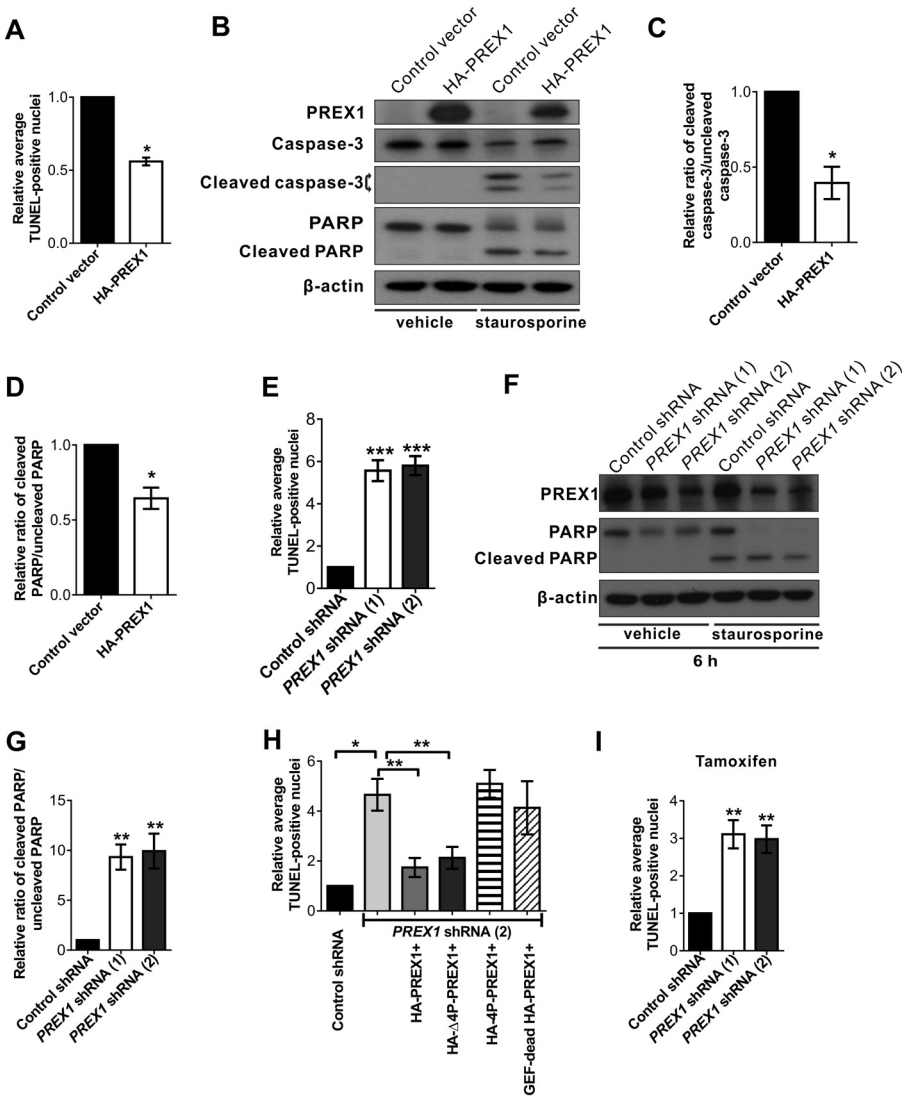

FIGURE 5. **PREX1 regulates staurosporine/tamoxifen-induced apoptosis.** *A*, stable MDA-MB-231-luc-D3H1 cells expressing control vector or HA-PREX1 were treated with 1 μM staurosporine for 16 h. Apoptotic cells were identified using a TUNEL assay. Data are presented as mean -fold change in TUNEL-positive cells ± S.E. relative to control vector, which was assigned an arbitrary value of 1 ($n = 3$). *B*, stable MDA-MB-231-luc-D3H1 cells expressing control vector or HA-PREX1 treated with DMSO vehicle or 1 μM staurosporine for 6 h were lysed and immunoblotted using PREX1, caspase 3, cleaved-caspase 3 (Asp^{175}), PARP, or β-actin antibodies. *C* and *D*, data are presented as mean -fold change in cleaved caspase-3/uncleaved caspase-3 (*C*) or cleaved PARP/uncleaved PARP (*D*) ± S.E. relative to control vector, which was assigned an arbitrary value of 1 ($n = 3$). *E*, MCF-7-luc-F5 cells expressing control shRNA, *PREX1* shRNA (1), or *PREX1* shRNA (2) were treated with 1 μM staurosporine for 16 h. Apoptotic cells were identified using a TUNEL assay. Data are presented as mean -fold change in TUNEL-positive cells ± S.E. relative to control shRNA, which was assigned an arbitrary value of 1 ($n = 3$). *F*, stable MCF-7-luc-F5 cells expressing control shRNA, *PREX1* shRNA (1), or *PREX1* shRNA (2) treated with DMSO vehicle or 1 μM staurosporine for 6 h were lysed and immunoblotted using PREX1, PARP, or β-actin antibodies. *G*, data are presented as mean -fold change in cleaved PARP/uncleaved PARP ± S.E. relative to control shRNA, which was assigned an arbitrary value of 1 ($n = 3$). *H*, stable MCF-7-luc-F5 cells expressing control shRNA, *PREX1* shRNA (2), *PREX1* shRNA (2) + HA-PREX1, *PREX1* shRNA (2) + HA-Δ4P-PREX1, *PREX1* shRNA (2) + HA-4P-PREX1, or *PREX1* shRNA (2) + GEF-dead HA-PREX1 were treated with 1 μM staurosporine for 16 h. Apoptotic cells were identified using a TUNEL assay. Data are presented as mean -fold change in TUNEL-positive cells ± S.E. relative to control shRNA, which was assigned an arbitrary value of 1 ($n = 3$). *I*, stable MCF-7-luc-F5 cells expressing control shRNA, *PREX1* shRNA (1), or *PREX1* shRNA (2) were treated with 3 μM tamoxifen for 16 h. Apoptotic cells were identified using a TUNEL assay. Data are presented as mean -fold increase in TUNEL-positive cells ± S.E. relative to control shRNA, which was assigned an arbitrary value of 1 ($n = 3$). *, $p < 0.05$; **, $p < 0.01$; ***, $p < 0.001$.

antibody staining was observed (Fig. 7, *E* and *H*). In contrast, *PREX1* shRNA knockdown MCF-7-luc-F5 cell xenografts in mammary fat pads showed a reduced rate of tumor growth compared with control shRNA tumors; however, tumor growth was not completely inhibited (Fig. 7, *I–K*), as reported previously (10, 11). *PREX1* knockdown tumors exhibited reduced numbers of proliferating cells by Ki-67 staining (Fig. 7, *L* and *M*) and reduced phosphorylated ERK1/2 antibody staining (Fig. 7, *L* and *N*).

Discussion

PREX1 is a critical effector of ErbB2/3 signaling in breast cancer (10, 11). PREX1 expression is essentially undetectable in normal human mammary epithelial tissue but is significantly up-regulated in human breast carcinomas, specifically the ER^+ luminal subtype (10, 11). The mechanisms underlying PREX1 promotion of cell proliferation and transformation are still emerging. Although several studies have examined the effects of *PREX1* shRNA knockdown on cell proliferation, anchorage-

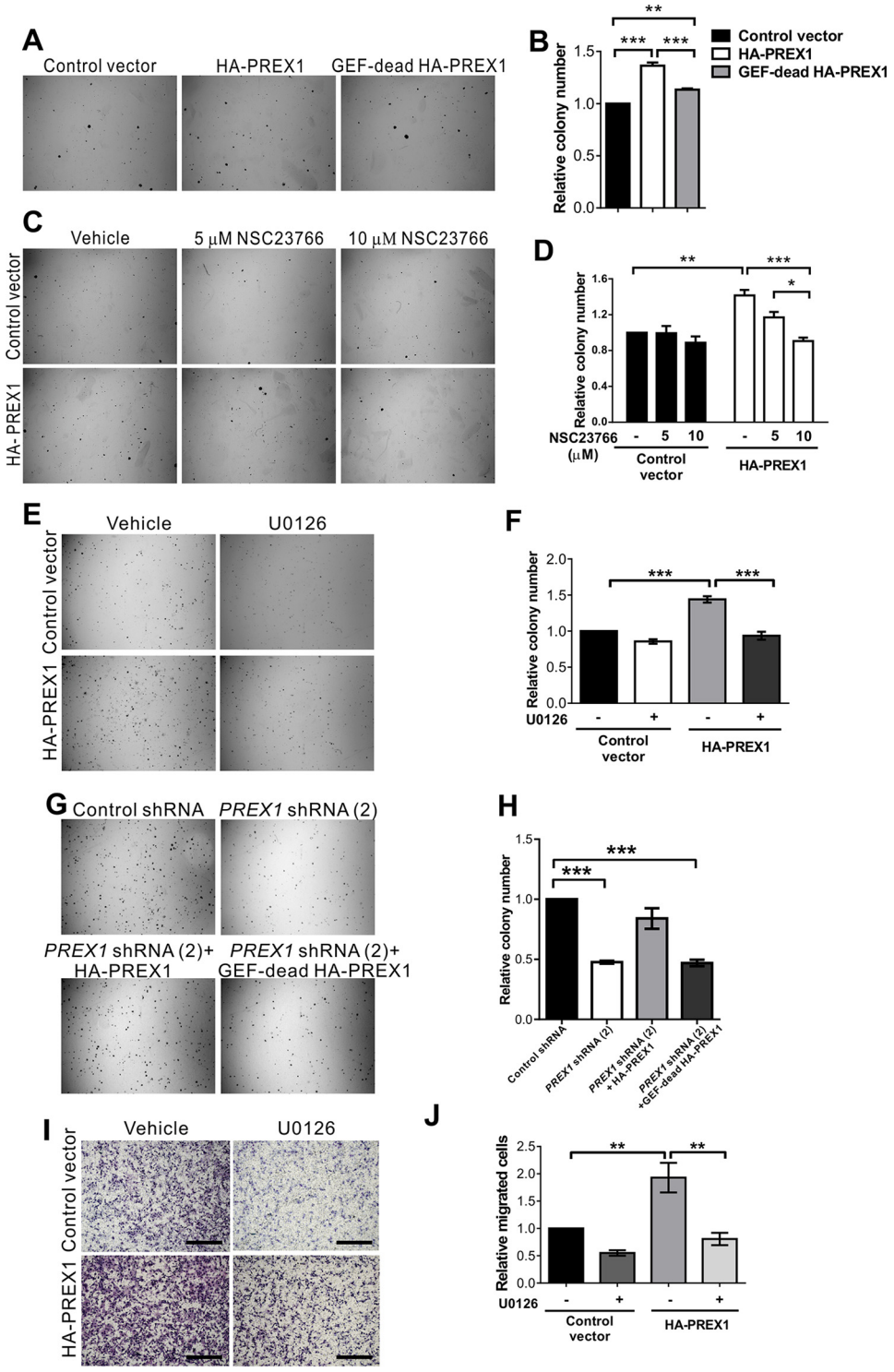

FIGURE 6. **PREX1-regulated anchorage-independent cell growth and cell migration is dependent on ERK1/2 activity.** *A*, stable MDA-MB-231-luc-D3H1 cells expressing control vector, HA-PREX1, or GEF-dead HA-PREX1 were grown in soft agar for 3–4 weeks. Representative images are shown. *B*, data are presented as mean -fold change in colony number ± S.E. relative to control vector, which was assigned an arbitrary value of 1 ($n = 3$). *C*, stable MDA-MB-231-luc-D3H1 cells expressing control vector or HA-PREX1 were grown in soft agar with addition of 5 or 10 μM NSC23766 (Rac1 inhibitor) or DMSO vehicle. *D*, data are presented as mean -fold change in colony number ± S.E. relative to vehicle-treated control vector, which was assigned an arbitrary value of 1 ($n = 4$). *E*, stable MDA-MB-231-luc-D3H1 cells expressing control vector or HA-PREX1 with addition of 1 μM U0126 (MEK1/2 inhibitor) or DMSO vehicle were grown in soft agar. *F*, data are presented as mean -fold change in colony number ± S.E. relative to control vector, which was assigned an arbitrary value of 1 ($n = 3$). *G*, stable MCF-7-luc-F5 cells expressing control shRNA, *PREX1* shRNA (2), *PREX1* shRNA (2) + HA-PREX1, or *PREX1* shRNA (2) + GEF-dead HA-PREX1 were grown in soft agar. *H*, data are presented as mean -fold change in colony number ± S.E. relative to control shRNA, which was assigned an arbitrary value of 1 ($n = 3$). *I*, the migration capacity of stable MDA-MB-231-luc-D3H1 cells expressing control vector or HA-PREX1 pretreated with DMSO vehicle or 20 μM U0126 was assessed by Transwell assay. Cells were allowed to migrate toward 10% FCS-containing growth medium. *J*, data are presented as mean -fold change in migrated cells ± S.E. relative to vehicle-treated control vector, which was assigned an arbitrary value of 1 ($n = 3$). *, $p < 0.05$; **, $p < 0.01$; ***, $p < 0.001$. *Scale bar* = 200 μm.

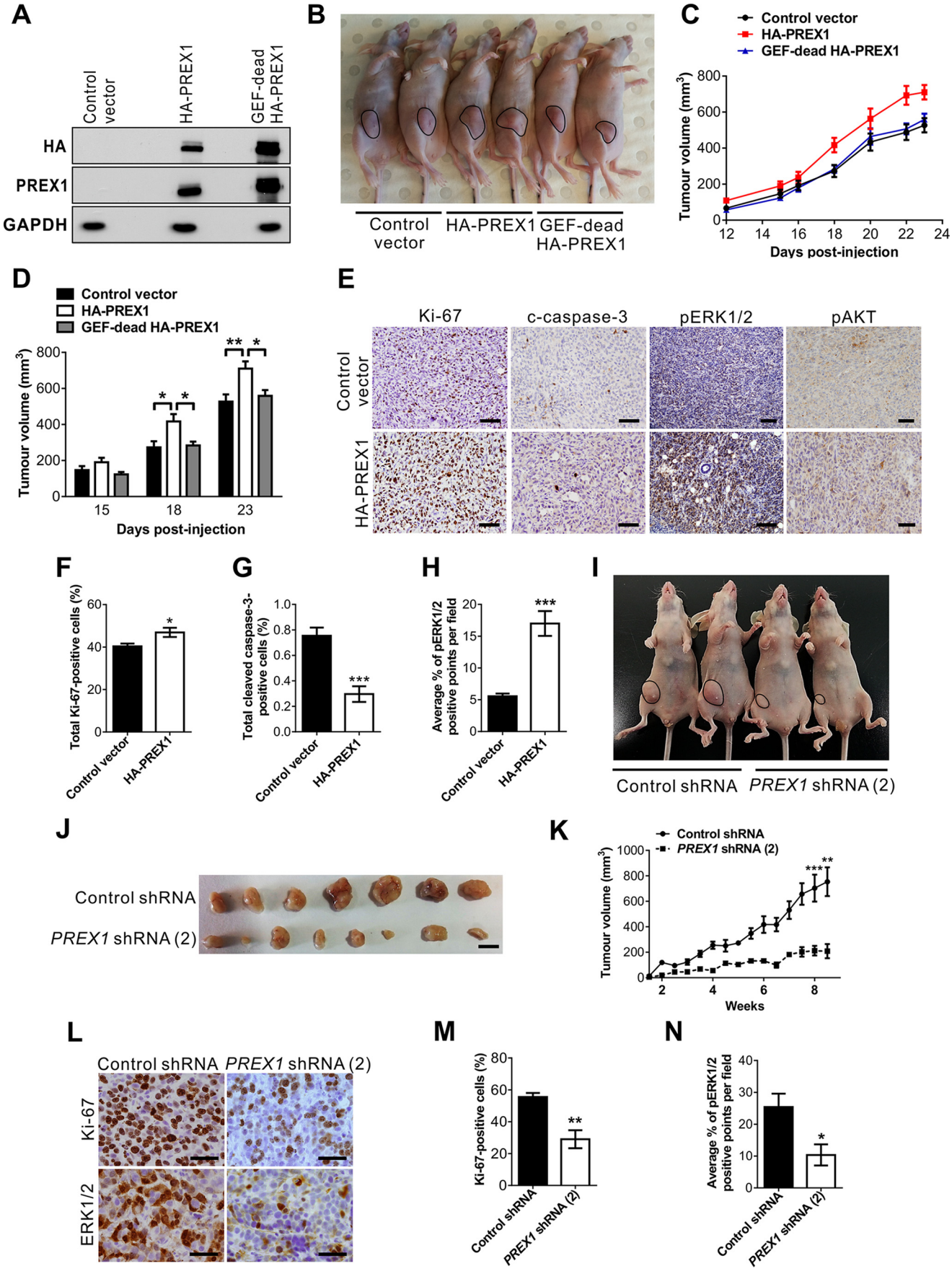

independent cell growth, and xenograft formation (10, 11, 19, 40), our study is the first to show that ERK1/2 is a critical downstream mediator of PREX1 oncogenicity in breast cancer. Here we report increased PREX1 expression promotes ERK1/2 phosphorylation, breast cancer cell proliferation, anchorage-independent cell growth, and xenograft tumor growth. In addition, PREX1 regulates apoptosis in response to staurosporine and, more significantly, the anti-estrogen drug tamoxifen. Although several studies have shown that PREX1 promotes ERK1/2 signaling in breast cancer cells (19, 40), evidence that this is a mechanism for its oncogenicity has not been shown. As reported here, inhibition of ERK1/2 signaling suppresses PREX1-driven anchorage-independent cell growth, cell migration, and inhibition of apoptosis. Furthermore, in a series of reconstitution experiments, we demonstrate that PREX1-mediated ERK1/2 activation and anchorage independent cell growth are critically dependent on PREX1 Rac-GEF activity.

PI3K-generated PtdIns(3,4,5)P_3 positively regulates PREX1 activation, which, in turn, activates AKT and ERK signaling in a positive feedback loop (5, 8, 19). In addition, the PI3K-activated Rac/PAK signaling pathway positively regulates the Raf-MEK1/2-ERK1/2 signaling cascade. Rac/PAK enhances ERK1/2 activation in breast cancer cells in response to prolactin stimulation in a PI3K-dependent but AKT-independent manner (41). Several models have proposed that PI3K activates PREX1, which, in turn, activates Rac/PAK, leading to the activation of ERK1/2 (19, 40), although the direct link between PREX1, Rac/PAK, and ERK1/2 signaling is yet to be established in breast cancer. As reported here, overexpression of PREX1 in breast cancer cells significantly enhanced ERK1/2 phosphorylation and the expression of its downstream effectors cyclin D1 and $p21^{WAF1/CIP1}$ but not phosphorylation of AKT. We also demonstrated PREX1 enhanced anchorage-independent cell growth in a Rac1- and MEK1/2-ERK1/2-dependent manner. PREX1-regulated cell proliferation was associated with the induction of cyclin D1 and $p21^{WAF1/CIP1}$ expression. In general, cyclin D1 is regarded as oncogenic because of its role in promoting cell cycle progression through the G_1-S phase transition (42), whereas $p21^{WAF1/CIP1}$ is a well established negative regulator of cell cycle progression (43). However, accumulating evidence suggests that $p21^{WAF1/CIP1}$ can positively regulate cell proliferation by protecting the degradation of cytoplasmic cyclin D1, leading to cyclin D1 retention in the nucleus and its association with cyclin-dependent kinase Cdk4/6 (44–46). A recent report has shown that Rac1 and ERK1/2-mediated breast cancer cell proliferation is associated with increased cyclin D1 and $p21^{WAF1/CIP1}$ protein expression following heregulin stimulation (21). Therefore, PREX1 regulation of cyclin D1 and $p21^{WAF1/CIP1}$ expression may depend on Rac1 and ERK1/2 activation; however, further investigation is required.

Here we showed that PREX1 overexpression or its shRNA knockdown in breast cancer cells did not significantly affect AKT phosphorylation/activation in response to EGF or IGF-1 stimulation. This is consistent with previous reports that AKT phosphorylation was not regulated by PREX1 following EGF, heregulin, or TGFα stimulation of human breast cancer cells (10). Nevertheless, we cannot exclude the possibility that PREX1 regulates AKT activation in other cancer cell types, as there is evidence that PREX1 promotes AKT phosphorylation via Rac1 in ovarian cancer cells (47), and a recent report showed that PREX1 promotes AKT phosphorylation in ER^+ breast cancer cells following IGF-1 stimulation (19). We observed a trend toward PREX1-regulated AKT activation, and it is possible that, with high agonist concentration, a more sustained activation of AKT may be observed.

Decreased xenograft mammary tumor growth has been described using *PREX1* shRNA in several breast cancer cell lines (10, 11), as also reported in this study. However, PREX1 expression is increased in human breast cancers, and no study has addressed whether overexpression of PREX1 *in vivo* can recapitulate these observations. Here we demonstrated, in a xenograft mouse model, that overexpression of wild-type but not GEF-dead PREX1 in MDA-MB-231-luc-D3H1 cells resulted in significantly larger tumors relative to control cells. In addition, tumors overexpressing PREX1 exhibited increased cell proliferation and reduced apoptosis and showed evidence of enhanced activation of ERK1/2 but not AKT, as demonstrated by phosphoimmunohistochemistry.

The Raf/MEK/ERK cascade is a key signaling pathway involved in regulating cell proliferation, survival, and migration (48); therefore, much attention has been focused on developing inhibitors of this signaling pathway. Not surprisingly, many of the available MEK inhibitors exhibit antitumor activity in human xenograft models of breast cancer, and some are currently undergoing phase I/II clinical trials (49, 50). It is tempting to speculate that breast cancers with PREX1 overexpression may benefit from therapeutic intervention of the Raf/MEK/ERK signaling pathway, although further studies are required to

FIGURE 7. **PREX1 promotes tumor growth and ERK1/2 phosphorylation in xenograft mouse models.** *A*, MDA-MB-231-luc-D3H1 cells stably transduced with control vector, HA-PREX1, or GEF-dead HA-PREX1 were analyzed by immunoblotting using HA, PREX1, or GAPDH antibodies. *B*, stable MDA-MB-231-luc-D3H1 cells expressing control vector, HA-PREX1, or GEF dead HA-PREX1 were injected into the mammary fat pads of BALB/c *nu/nu* mice, and tumor growth was analyzed by caliper measurement. *C*, measurement of tumor size over 23 days. The mean tumor volume ± S.E. of seven (control vector, GEF dead HA-PREX1) or eight (HA-PREX1) individual animals per group is shown. *D*, mean tumor volumes 15, 18, and 23 days post-injection indicate that HA-PREX1-overexpressing cells form larger tumors *in vivo*. *E*, control vector and HA-PREX1 tumors were immunostained using Ki-67, cleaved caspase-3, pERK1/2, or $pAKT^{Ser\text{-}473}$ antibodies. *Scale bar* = 100 μm. *F* and *G*, data represent the average percentage of Ki-67-positive (*F*) or cleaved caspase-3-positive cells (*G*) ± S.E. 5 fields/tumor were examined, and 5 animals/group were analyzed. *H*, the number of pERK1/2-positive points per field of 5 fields/tumor was determined and expressed as a percentage of total points per field. Data represent the average percentage of pERK1/2-positive points per field ± S.E. 5 animals/group were analyzed. *I*, stable MCF-7-luc-F5 cells expressing control shRNA or *PREX1* shRNA (2) were injected into the mammary fat pads of BALB/c *nu/nu* mice, and tumor growth was analyzed by caliper measurement. *J*, photograph of tumors extracted 8.5 weeks post-injection shows that *PREX1* shRNA (2) cells formed smaller tumors compared with control shRNA cells. *Scale bar* = 1 cm. *K*, measurement of tumor size over 8.5 weeks. The mean tumor volume ± S.E. of seven control shRNA and eight *PREX1* shRNA (2) tumors is shown. *L*, control shRNA or *PREX1* shRNA (2) tumors were immunostained using Ki-67 or pERK1/2 antibodies. *Scale bar* = 50 μm. *M*, data represent the average percentage of Ki-67-positive cells ± S.E. 5 fields/sample were examined, and seven control shRNA and eight *PREX1* shRNA (2) tumors were analyzed. *N*, the number of pERK1/2-positive points per field of 5 fields/tumor were determined and expressed as a percentage of total points per field. Data represent the average percentage of pERK1/2-positive points per field ± S.E. Seven control shRNA and eight *PREX1* shRNA (2) tumors were analyzed. *, $p < 0.05$; **, $p < 0.01$; ***, $p < 0.001$.

evaluate these inhibitors in mouse breast cancer models with PREX1 overexpression.

Recently we reported the 1.95-Å x-ray crystal structure of the PREX1 DH-PH domain in complex with its canonical GTPase, Rac1 (51). Using structure-guided mutagenesis, we dissected the critical role the PREX1 DH domain-Rac1 interface plays in promoting Rac1 activation both *in vitro* and downstream of G-protein-coupled receptor and receptor tyrosine kinase signaling in breast cancer cell lines (51). Here we demonstrated that the PREX1 DH-PH domain is also critical in mediating PREX1 anchorage-independent cell growth and inhibition of apoptosis. Other domains, such as the IP4P domain, exhibit no activity in this context. Notably, PREX1-mediated cell growth/survival under anchorage-independent conditions and xenograft tumor growth are dependent on its ability to activate Rac, suggesting that regulation of this signaling pathway may be a potential mechanism for targeted therapies for PREX1-positive tumors.

Experimental Procedures

Cell Lines and Antibodies—MCF-7-luc-F5 (MCF-7 human mammary adenocarcinoma cells stably transfected with the North American firefly luciferase gene expressed from a CMV promoter) and MDA-MB-231-luc-D3H1 (MDA-MB-231 human mammary adenocarcinoma cells stably transfected with the North American firefly luciferase gene expressed from an SV40 promoter) breast cancer cell lines were purchased from Caliper Life Sciences (PerkinElmer Life Sciences).

Antibodies for ERK1/2 (4695), pERK1/2 (9106), β-actin (4970), AKT (4685), pAKT$^{Thr\text{-}308}$ (4056), pAKT$^{Ser\text{-}473}$ (4058), caspase-3 (9665), cleaved caspase-3 (Asp^{157}, 9664) and PARP (9532) were purchased from Cell Signaling Technology (Boston, MA). Ki-67 (RM-9106-S0) and GAPDH (AM4300) antibodies were purchased from Thermo Fisher (Waltham, MA). Monoclonal HA antibody (MMS-101R) was purchased from Covance (Princeton, NJ). PREX1 antibodies were generated in-house and purified against recombinant EE-PREX1 protein.

Cell Culture and Lentiviral Transductions—MDA-MB-231-luc-D3H1 cells were maintained in DMEM (Gibco, Life Technologies) supplemented with 10% FBS (Gibco, Life Technologies), 100 units/ml penicillin, 1% (v/v) streptomycin, and 2 mM L-glutamine (JRH Biosciences, St. Louis, MO). MCF-7-luc-F5 cells were maintained as described above with addition of 10 μg/ml human insulin (Sigma-Aldrich). Heterogeneous pools of MDA-MB-231-luc-D3H1 cells stably expressing HA-PREX1, GEF-dead HA-PREX1, or control vector (mCherry) were generated by transduction with lentiviral particles carrying the plasmid pHIV-1SDmCMVmCherry.pre encoding control vector alone, HA-PREX1, or GEF-dead HA-PREX1. Heterogeneous pools of *PREX1* knockdown MCF-7-luc-F5 cells were generated by transducing non-target shRNA or two shRNA sequences targeting two distinct regions of *PREX1* mRNA (Sigma-Aldrich, St. Louis, MO). Clones were selected in complete medium containing 1 μg/ml puromycin for 1 week and then maintained in 0.5 μg/ml of puromycin. Heterogeneous pools of *PREX1* knockdown MCF-7-luc-F5 cells stably expressing lentiviral particles carrying the plasmid pHIV-1SDmCMVmCherry.pre encoding HA-PREX1, Δ4P-PREX1, 4P-PREX1, or GEF-dead-PREX1 were generated as described above.

Western Blotting—For EGF or IGF-1-stimulation assays, cells were serum-starved for 24 h before stimulation with 100 ng/ml EGF (BD Biosciences) or 10 ng/ml IGF-1 (Sigma-Aldrich). MCF-7-luc-F5 cells were serum-starved in phenol-red free DMEM (Gibco, Life Technologies). Cells were lysed in SDS-PAGE sample buffer (62.5 mM Tris-HCl (pH 6.8), 2% (w/v) SDS, 10% glycerol, 50 mM DTT, and 0.01% (w/v) bromphenol blue). To analyze the protein expression of cleaved caspase-3 or PARP, cells were treated with 1 μM staurosporine (Cell Signaling Technology) for 6 h and then lysed with ice-cold lysis buffer (1% Triton X-100, 20 mM Tris-HCl (pH 7.4), 150 mM NaCl, and a protease mixture tablet (Roche)). Equal amounts of total protein were separated by 10% SDS-PAGE followed by immunoblotting, and then signals were visualized by ECL (PerkinElmer Life Sciences). Commercially available antibodies were used at dilutions according to the recommendations of the manufacturer. In-house affinity-purified polyclonal PREX1 antibodies were used at 1:1000.

Soft Agar Assay—6×10^3 cells were resuspended in DMEM/10% FBS/0.3% agar with addition of 1 μM U0126 (Cell Signaling Technology), 5 or 10 μM NSC23766 (Tocris Bioscience), or DMSO over a base composed of DMEM/10% FBS/0.7% agar in 6-well dishes in triplicate for each experiment. Cells were incubated for 3–4 weeks at 37 °C, and then colonies were imaged using a Leica M165C stereomicroscope and a Leica DFC295 camera.

In Vitro Cell Proliferation Assays—For MTT assays, equal numbers of cells were seeded into 96-well plates and incubated for 0, 24, 48, or 72 h. Cell proliferation assays were performed using the Cell Proliferation Kit I (MTT, Roche) according to the instructions of the manufacturer.

TUNEL Assay—Apoptosis was induced by addition of 1 μM staurosporine (Cell Signaling Technology) or 3 μM tamoxifen (Sigma-Aldrich) to complete medium for 16 h. Cells were fixed with 3–4% paraformaldehyde for 1 h. Apoptotic cells were identified using the *In Situ* Cell Death Detection Kit, Fluorescein (Roche) according to the instructions of the manufacturer. Five random fields per coverslip were imaged, and >250 cells/coverslip were counted.

Orthotopic Xenograft Implantation—All experimental procedures involving mice were approved by the Animal Ethics Committee at the Monash University School of Biomedical Sciences (SOBS/2008/14 or MARP/2013/132). A total of 1×10^6 cells suspended in 15 μl of PBS plus 50% growth factor-reduced Matrigel (BD Biosciences) were injected into the mammary fat pads of 7- to 8-week-old female BALB/c *nu/nu* mice (Animal Resources Centre, Australia). Mice injected with MCF-7-luc-F5 cells were also implanted with 90-day release, 1.7-mg/ml E_2 pellets (Innovative Research of America) under anesthesia. The width and length of palpable tumors were measured with digital calipers three times weekly. Tumor volume was calculated using the equation (length) x $(\text{width})^2/2$.

Immunohistochemistry—Xenograft tumors were excised, fixed in 10% formalin overnight, and then paraffin-embedded. Tumor sections were deparaffinized in three changes of xylene, rehydrated through three changes of ethanol, and then sub-

jected to heat-induced antigen retrieval for 10 min in EDTA (pH 9.0). Tumor sections were blocked with 1% BSA before incubation with p-ERK1/2, cleaved caspase-3 (Asp^{175}), or Ki-67 antibodies diluted in 1% BSA at 4 °C overnight. Primary antibodies were used at dilutions according to the recommendations of the manufacturer. Immunoreactivity was detected using the EnVision+ HRP-3,3′-diaminobenzidine system (Dako, Glostrup, Denmark) according to the instructions of the manufacturer. Coverslips were mounted using D.P.X. (Sigma-Aldrich). 3,3′-diaminobenzidine staining of p-ERK1/2 was quantified by counting the p-ERK1/2-positive points of five different fields/tumor using ImageJ analysis software.

Boyden Chamber Migration Assay—Cell migration assays were performed using 6.5-mm Transwells with 8.0-μm pore polycarbonate membrane inserts (Corning). Cells were serum-starved for 48 h before being seeded in the upper chamber in serum-free medium containing DMSO or U0126 for 5 h at 37 °C. Complete medium was placed in the lower compartment as a chemoattractant. After incubation, non-migrated cells were wiped off from the upper surface with a cotton swab, and migrated cells on the lower surface were fixed and stained using the DiffQuick staining kit (Lab Aids Pty Ltd., Narrabeen, Australia). All migrated cells were counted and quantified using ImageJ analysis software.

Statistical Analysis—All Statistical analyses were performed using GraphPad Prism 5.0 by unpaired Student's t test or one-way analysis of variance followed by Dunnett's post-test. $p < 0.05$ was considered statistically significant.

Author Contributions—H. J. L., L. M. O., N. S., J. M., and J. E. W. performed experiments. J. V. and J. T. P. performed the mouse xenograft experiments. Y. F., C. G. B., and J. E. J. R. generated the plasmids and lentiviral particles. H. J. L., L. M. O., N. S., and J. T. P. contributed to the experimental design and data analysis. C. A. M. formulated the hypotheses, designed the experiments, and analyzed the data. The manuscript was written by H. J. L. and C. A. M. and edited by all authors.

Acknowledgments—We thank Prof. Tony Tiganis for helpful discussions and advice and Dr. Sandra Feeney, Dr. Rajendra Gurung, and Dr. Absorn Sriratana for technical assistance. This study utilized the Monash Micro Imaging Facility, Monash University, Victoria, Australia.

References

1. Jaffe, A. B., and Hall, A. (2005) Rho GTPases: biochemistry and biology. *Annu. Rev. Cell Dev. Biol.* **21,** 247–269
2. Orgaz, J. L., Herraiz, C., and Sanz-Moreno, V. (2014) Rho GTPases modulate malignant transformation of tumor cells. *Small GTPases* **5,** e29019
3. Sadok, A., and Marshall, C. J. (2014) Rho GTPases: masters of cell migration. *Small GTPases* **5,** e29710
4. Rossman, K. L., Der, C. J., and Sondek, J. (2005) GEF means go: turning on RHO GTPases with guanine nucleotide-exchange factors. *Nat. Rev. Mol. Cell Biol.* **6,** 167–180
5. Welch, H. C., Coadwell, W. J., Ellson, C. D., Ferguson, G. J., Andrews, S. R., Erdjument-Bromage, H., Tempst, P., Hawkins, P. T., and Stephens, L. R. (2002) P-Rex1, a PtdIns(3,4,5)P3- and G$\beta\gamma$-regulated guanine-nucleotide exchange factor for Rac. *Cell* **108,** 809–821
6. Welch, H. C., Condliffe, A. M., Milne, L. J., Ferguson, G. J., Hill, K., Webb, L. M., Okkenhaug, K., Coadwell, W. J., Andrews, S. R., Thelen, M., Jones, G. E., Hawkins, P. T., and Stephens, L. R. (2005) P-Rex1 regulates neutrophil function. *Curr. Biol.* **15,** 1867–1873
7. Lawson, C. D., Donald, S., Anderson, K. E., Patton, D. T., and Welch, H. C. (2011) P-Rex1 and Vav1 cooperate in the regulation of formyl-methionyl-leucyl-phenylalanine-dependent neutrophil responses. *J. Immunol.* **186,** 1467–1476
8. Hill, K., Krugmann, S., Andrews, S. R., Coadwell, W. J., Finan, P., Welch, H. C., Hawkins, P. T., and Stephens, L. R. (2005) Regulation of P-Rex1 by phosphatidylinositol (3,4,5)-trisphosphate and G$\beta\gamma$ subunits. *J. Biol. Chem.* **280,** 4166–4173
9. Rynkiewicz, N. K., Liu, H. J., Balamatsias, D., and Mitchell, C. A. (2012) INPP4A/INPP4B and P-Rex proteins: related but different? *Adv. Biol. Regul.* **52,** 265–279
10. Sosa, M. S., Lopez-Haber, C., Yang, C., Wang, H., Lemmon, M. A., Busillo, J. M., Luo, J., Benovic, J. L., Klein-Szanto, A., Yagi, H., Gutkind, J. S., Parsons, R. E., and Kazanietz, M. G. (2010) Identification of the Rac-GEF P-Rex1 as an essential mediator of ErbB signaling in breast cancer. *Mol. Cell* **40,** 877–892
11. Montero, J. C., Seoane, S., Ocaña, A., and Pandiella, A. (2011) P-Rex1 participates in Neuregulin-ErbB signal transduction and its expression correlates with patient outcome in breast cancer. *Oncogene* **30,** 1059–1071
12. Fine, B., Hodakoski, C., Koujak, S., Su, T., Saal, L. H., Maurer, M., Hopkins, B., Keniry, M., Sulis, M. L., Mense, S., Hibshoosh, H., and Parsons, R. (2009) Activation of the PI3K pathway in cancer through inhibition of PTEN by exchange factor P-REX2a. *Science* **325,** 1261–1265
13. Lindsay, C. R., Lawn, S., Campbell, A. D., Faller, W. J., Rambow, F., Mort, R. L., Timpson, P., Li, A., Cammareri, P., Ridgway, R. A., Morton, J. P., Doyle, B., Hegarty, S., Rafferty, M., Murphy, I. G., *et al.* (2011) P-Rex1 is required for efficient melanoblast migration and melanoma metastasis. *Nat. Commun.* **2,** 555
14. Barrio-Real, L., and Kazanietz, M. G. (2012) Rho GEFs and cancer: linking gene expression and metastatic dissemination. *Sci. Signal* **5,** pe43
15. Asimakopoulos, F. A., and Green, A. R. (1996) Deletions of chromosome 20q and the pathogenesis of myeloproliferative disorders. *Br. J. Haematol.* **95,** 219–226
16. Berry, R., Schroeder, J. J., French, A. J., McDonnell, S. K., Peterson, B. J., Cunningham, J. M., Thibodeau, S. N., and Schaid, D. J. (2000) Evidence for a prostate cancer-susceptibility locus on chromosome 20. *Am. J. Hum. Genet.* **67,** 82–91
17. Stumpf, E., Aalto, Y., Höög, A., Kjellman, M., Otonkoski, T., Knuutila, S., and Andersson, L. C. (2000) Chromosomal alterations in human pancreatic endocrine tumors. *Genes Chromosomes Cancer* **29,** 83–87
18. Larramendy, M. L., Lushnikova, T., Björkqvist, A. M., Wistuba, I. I., Virmani, A. K., Shivapurkar, N., Gazdar, A. F., and Knuutila, S. (2000) Comparative genomic hybridization reveals complex genetic changes in primary breast cancer tumors and their cell lines. *Cancer Genet. Cytogenet.* **119,** 132–138
19. Dillon, L. M., Bean, J. R., Yang, W., Shee, K., Symonds, L. K., Balko, J. M., McDonald, W. H., Liu, S., Gonzalez-Angulo, A. M., Mills, G. B., Arteaga, C. L., and Miller, T. W. (2015) P-REX1 creates a positive feedback loop to activate growth factor receptor, PI3K/AKT and MEK/ERK signaling in breast cancer. *Oncogene* **34,** 3968–3976
20. Campbell, A. D., Lawn, S., McGarry, L. C., Welch, H. C., Ozanne, B. W., and Norman, J. C. (2013) P-Rex1 cooperates with PDGFRβ to drive cellular migration in 3D microenvironments. *PLoS ONE* **8,** e53982
21. Yang, C., Liu, Y., Lemmon, M. A., and Kazanietz, M. G. (2006) Essential role for Rac in heregulin β1 mitogenic signaling: a mechanism that involves epidermal growth factor receptor and is independent of ErbB4. *Mol. Cell Biol.* **26,** 831–842
22. Yang, C., Klein, E. A., Assoian, R. K., and Kazanietz, M. G. (2008) Heregulin β1 promotes breast cancer cell proliferation through Rac/ERK-dependent induction of cyclin D1 and p21Cip1. *Biochem. J.* **410,** 167–175
23. Lewis-Saravalli, S., Campbell, S., and Claing, A. (2013) ARF1 controls Rac1 signaling to regulate migration of MDA-MB-231 invasive breast cancer cells. *Cell Signal* **25,** 1813–1819
24. Morimura, S., and Takahashi, K. (2011) Rac1 and stathmin but not EB1 are required for invasion of breast cancer cells in response to IGF-I. *Int. J. Cell Biol.* **2011,** 615912

25. Duncia, J. V., Santella, J. B., 3rd, Higley, C. A., Pitts, W. J., Wityak, J., Frietze, W. E., Rankin, F. W., Sun, J. H., Earl, R. A., Tabaka, A. C., Teleha, C. A., Blom, K. F., Favata, M. F., Manos, E. J., Daulerio, A. J., *et al.* (1998) MEK inhibitors: the chemistry and biological activity of U0126, its analogs, and cyclization products. *Bioorg. Med. Chem. Lett.* **8,** 2839–2844
26. Favata, M. F., Horiuchi, K. Y., Manos, E. J., Daulerio, A. J., Stradley, D. A., Feeser, W. S., Van Dyk, D. E., Pitts, W. J., Earl, R. A., Hobbs, F., Copeland, R. A., Magolda, R. L., Scherle, P. A., and Trzaskos, J. M. (1998) Identification of a novel inhibitor of mitogen-activated protein kinase kinase. *J. Biol. Chem.* **273,** 18623–18632
27. Albanese, C., Johnson, J., Watanabe, G., Eklund, N., Vu, D., Arnold, A., and Pestell, R. G. (1995) Transforming p21ras mutants and c-Ets-2 activate the cyclin D1 promoter through distinguishable regions. *J. Biol. Chem.* **270,** 23589–23597
28. Lavoie, J. N., L'Allemain, G., Brunet, A., Müller, R., and Pouysségur, J. (1996) Cyclin D1 expression is regulated positively by the p42/p44MAPK and negatively by the p38/HOGMAPK pathway. *J. Biol. Chem.* **271,** 20608–20616
29. Sherr, C. J. (1994) G_1 phase progression: cycling on cue. *Cell* **79,** 551–555
30. Dyson, N. (1998) The regulation of E2F by pRB-family proteins. *Genes Dev.* **12,** 2245–2262
31. Liu, Y., Martindale, J. L., Gorospe, M., and Holbrook, N. J. (1996) Regulation of p21WAF1/CIP1 expression through mitogen-activated protein kinase signaling pathway. *Cancer Res.* **56,** 31–35
32. Zezula, J., Sexl, V., Hutter, C., Karel, A., Schütz, W., and Freissmuth, M. (1997) The cyclin-dependent kinase inhibitor p21cip1 mediates the growth inhibitory effect of phorbol esters in human venous endothelial cells. *J. Biol. Chem.* **272,** 29967–29974
33. Ooms, L. M., Binge, L. C., Davies, E. M., Rahman, P., Conway, J. R., Gurung, R., Ferguson, D. T., Papa, A., Fedele, C. G., Vieusseux, J. L., Chai, R. C., Koentgen, F., Price, J. T., Tiganis, T., Timpson, P., *et al.* (2015) The inositol polyphosphate 5-phosphatase PIPP regulates AKT1-dependent breast cancer growth and metastasis. *Cancer Cell* **28,** 155–169
34. Ajabnoor, G. M., Crook, T., and Coley, H. M. (2012) Paclitaxel resistance is associated with switch from apoptotic to autophagic cell death in MCF-7 breast cancer cells. *Cell Death Disease* **3,** e260
35. Manns, J., Daubrawa, M., Driessen, S., Paasch, F., Hoffmann, N., Löffler, A., Lauber, K., Dieterle, A., Alers, S., Iftner, T., Schulze-Osthoff, K., Stork, B., and Wesselborg, S. (2011) Triggering of a novel intrinsic apoptosis pathway by the kinase inhibitor staurosporine: activation of caspase-9 in the absence of Apaf-1. *FASEB J.* **25,** 3250–3261
36. Bianchi-Smiraglia, A., Paesante, S., and Bakin, A. V. (2013) Integrin $\beta5$ contributes to the tumorigenic potential of breast cancer cells through the Src-FAK and MEK-ERK signaling pathways. *Oncogene* **32,** 3049–3058
37. Faivre, E. J., and Lange, C. A. (2007) Progesterone receptors upregulate Wnt-1 to induce epidermal growth factor receptor transactivation and c-Src-dependent sustained activation of Erk1/2 mitogen-activated protein kinase in breast cancer cells. *Mol. Cell Biol.* **27,** 466–480
38. Qin, J., Xie, Y., Wang, B., Hoshino, M., Wolff, D. W., Zhao, J., Scofield, M. A., Dowd, F. J., Lin, M. F., and Tu, Y. (2009) Upregulation of PIP3-dependent Rac exchanger 1 (P-Rex1) promotes prostate cancer metastasis. *Oncogene* **28,** 1853–1863
39. Reddy, K. B., Nabha, S. M., and Atanaskova, N. (2003) Role of MAP kinase in tumor progression and invasion. *Cancer Metastasis Rev.* **22,** 395–403
40. Ebi, H., Costa, C., Faber, A. C., Nishtala, M., Kotani, H., Juric, D., Della Pelle, P., Song, Y., Yano, S., Mino-Kenudson, M., Benes, C. H., and Engelman, J. A. (2013) PI3K regulates MEK/ERK signaling in breast cancer via the Rac-GEF, P-Rex1. *Proc. Natl. Acad. Sci. U.S.A.* **110,** 21124–21129
41. Aksamitiene, E., Achanta, S., Kolch, W., Kholodenko, B. N., Hoek, J. B., and Kiyatkin, A. (2011) Prolactin-stimulated activation of ERK1/2 mitogen-activated protein kinases is controlled by PI3-kinase/Rac/PAK signaling pathway in breast cancer cells. *Cell Signal.* **23,** 1794–1805
42. Knudsen, K. E., Diehl, J. A., Haiman, C. A., and Knudsen, E. S. (2006) Cyclin D1: polymorphism, aberrant splicing and cancer risk. *Oncogene* **25,** 1620–1628
43. el-Deiry, W. S., Tokino, T., Velculescu, V. E., Levy, D. B., Parsons, R., Trent, J. M., Lin, D., Mercer, W. E., Kinzler, K. W., and Vogelstein, B. (1993) WAF1, a potential mediator of p53 tumor suppression. *Cell* **75,** 817–825
44. LaBaer, J., Garrett, M. D., Stevenson, L. F., Slingerland, J. M., Sandhu, C., Chou, H. S., Fattaey, A., and Harlow, E. (1997) New functional activities for the p21 family of CDK inhibitors. *Genes Dev.* **11,** 847–862
45. Roninson, I. B. (2002) Oncogenic functions of tumour suppressor p21(Waf1/Cip1/Sdi1): association with cell senescence and tumour-promoting activities of stromal fibroblasts. *Cancer Lett.* **179,** 1–14
46. Weiss, R. H. (2003) p21Waf1/Cip1 as a therapeutic target in breast and other cancers. *Cancer Cell* **4,** 425–429
47. Kim, E. K., Yun, S. J., Ha, J. M., Kim, Y. W., Jin, I. H., Yun, J., Shin, H. K., Song, S. H., Kim, J. H., Lee, J. S., Kim, C. D., and Bae, S. S. (2011) Selective activation of Akt1 by mammalian target of rapamycin complex 2 regulates cancer cell migration, invasion, and metastasis. *Oncogene* **30,** 2954–2963
48. Kim, E. K., and Choi, E. J. (2010) Pathological roles of MAPK signaling pathways in human diseases. *Biochim. Biophys. Acta* **1802,** 396–405
49. Iverson, C., Larson, G., Lai, C., Yeh, L. T., Dadson, C., Weingarten, P., Appleby, T., Vo, T., Maderna, A., Vernier, J. M., Hamatake, R., Miner, J. N., and Quart, B. (2009) RDEA119/BAY 869766: a potent, selective, allosteric inhibitor of MEK1/2 for the treatment of cancer. *Cancer Res.* **69,** 6839–6847
50. Thompson, D. S., Flaherty, K., Messersmith, W., Harlacker, K., Nallapareddy, S., Vincent, C., DeMarini, D. J., Cox, D. S., O'Neill, V. J., and Burris, H. A. (2009) A three-part, phase I, dose-escalation study of GSK1120212, a potent MEK inhibitor, administered orally to subjects with solid tumors or lymphoma. *J. Clin. Oncol.* **27,** e14584
51. Lucato, C. M., Halls, M. L., Ooms, L. M., Liu, H. J., Mitchell, C. A., Whisstock, J. C., and Ellisdon, A. M. (2015) The phosphatidylinositol (3,4,5)-trisphosphate-dependent Rac exchanger 1·Ras-related C3 botulinum toxin substrate 1 (P-Rex1·Rac1) complex reveals the basis of Rac1 activation in breast cancer cells. *J. Biol. Chem.* **290,** 20827–20840

PtdIns(3,4,5)P_3-dependent Rac Exchanger 1 (PREX1) Rac-Guanine Nucleotide Exchange Factor (GEF) Activity Promotes Breast Cancer Cell Proliferation and Tumor Growth via Activation of Extracellular Signal-regulated Kinase 1/2 (ERK1/2) Signaling

Heng-Jia Liu, Lisa M. Ooms, Nuthasuda Srijakotre, Joey Man, Jessica Vieusseux, JoAnne E. Waters, Yue Feng, Charles G. Bailey, John E. J. Rasko, John T. Price and Christina A. Mitchell

J. Biol. Chem. 2016, 291:17258-17270.
doi: 10.1074/jbc.M116.743401 originally published online June 29, 2016
